RESEARCH   **Open Access**

Conventional ultrasound, color Doppler, TI-RADS, and shear wave elastography for thyroid nodule differentiation: a study of efficacy compared with the histopathology results

Ahmed Abd Alrahman Baz[1*], Afaf Hamdy Ibrahim Mohamed[1], Yasmine Fathy Ghazi El-Esawy[2] and Khaled Helmy El-kaffas[1]

Abstract

Background: Although a minority of the thyroid nodules is malignant, usually the invasive diagnostic procedures are warranted. This prospective study aims to assess the diagnostic performance of the US criteria in addition to the TI-RADS score and the SWE for the differentiation between the benign and malignant thyroid nodules as a potential surrogate for the invasive procedures.

Results: Ninety-nine patients with thyroid nodules (79 females and 20 males, with a mean age of 45.9 ± 7.7 years; 30–69 years) were enrolled in this study and underwent conventional ultrasound, color Doppler, TI-RADS scoring, and shear wave elastography (SWE); the findings were correlated to the histopathological results.
Our results revealed a significant increase in SWE elasticity indices (EIs) and presence of color Doppler signals in malignant nodules as compared with the benign ones ($p < 0.05$). Combined TI-RADS and SWE as well as TI-RADS and color Doppler imaging had given a better sensitivity for detection of malignancy.

Conclusion: Elasticity indices had shown a significantly high diagnostic performance that is almost approaching the histopathological results. Combined SWE, color Doppler and TI-RADS, as a sum of findings, could effectively differentiate between benign and malignant thyroid nodules. Furthermore, it had offered a non-invasive tool for accurate risk stratification of malignant nodules.

Keywords: Thyroid Nodules, Ultrasound, Shear wave elastography, Fine needle aspiration

Background

Thyroid nodules are commonly encountered clinical and radiological findings in the clinical practice; however, only minorities (less than 5%) of them are truly malignant and need further evaluation [1–5].

In the past, the assessment of the thyroid nodules used to be done by clinical examination, ultrasound, and radioisotopic scanning. Nonetheless, the cytological assessment by either fine-needle aspiration cytology (FNAC) or biopsy is often needed to preclude malignancy [3, 4].

The clinical examination per se cannot give a final diagnosis and usually, the US examination is requested; thus, some ultrasound criteria were employed for categorization of the suspicious nodules. A scoring system known as thyroid imaging reporting and data system (TI-RADS) has been validated, widely used, and updated in this regard [3, 5, 6].

* Correspondence: ahmedbaz2012@yahoo.com
[1]Radiology Department, Faculty of Medicine, Cairo University, Cairo, Egypt
Full list of author information is available at the end of the article

Elastography has been added as an ultrasound-based technique including the strain and the shear wave elastography (SWE) for getting an objective assessment of the tissue stiffness in organs like the liver and the breast lesions; nevertheless; the diagnostic accuracy of the thyroid elastography in malignancy detection is still controversial in the literature [5, 6].

Recently, functional imaging like diffusion-weighted MRI (DW-MRI) has been investigated for assessing thyroid malignancies as well as their recurrences, and it had reported fairly good results, but MRI has some limitations being contraindicated in claustrophobic patients and those with cardiac pacemakers; moreover, it is more expensive compared with the US [7, 8].

Eventually, some studies had investigated the use of SWE as a potential surrogate for invasive procedures (like FNAC) in the evaluation of soft thyroid nodules [9].

This prospective study aims to assess the diagnostic performance of the US criteria in addition to the TI-RADS score, and the SWE for differentiation between the benign and malignant thyroid nodules in patients referred for FNAC and to correlate the imaging patterns and the obtained values of the lesions with their histopathological results as a reference standard.

Methods

Subjects

This study had enrolled 99 patients with thyroid nodules who were referred to US or intervention units in our institute from the outpatient clinics, and the inpatient departments within the period from January 2019 to August 2020, there were 79 females and 20 males having a mean age of 45.92 ± 7.7 years (30–69 years).

Table 1 Showing the diagnostic performance of conventional B-mode and color Doppler characteristics of the nodules

Us features		Malignant	Benign	Sensitivity (%) or chi squared, t value[a]	Specificity (%) or p value
Nodule size in mm		27.7 ± 6.9	29.4 ± 4.1	$t = 1.5$	$p = 0.125$
Number of nodule	Solitary nodule	27	47	Chi squared = 1.3	0.252
	Multiple nodules[a]	6	19		
Location of the nodule					
	Right lobe	11	22	Chi squared = 0.060	p value = 0.996
	Left lobe	17	33		
	Isthmus	3	7		
	Different	2	4		
Composition	Solid ($n = 75$)	30	45	90.9	31.8
	Partially solid ($n = 24$)	3	21		
Echogenicity	Hypo or marked hypoechogenicity ($n = 28$)	22	6	66.6	90.9
	Hyper or isoechogenicity ($n = 71$)	11	60		
Calcification	Microcalcification ($n = 12$)	12	0	36.3	10
	Macro or no calcification ($n = 87$)	21	66		
Shape	Taller than wider ($n = 4$)	4	0	12.1	10
	Wider than taller ($n = 95$)	29	66		
Margin	Irregular/ lobulated ($n = 13$)	2	11	6.06	83.3
	Smooth/ill-defined ($n = 86$)	31	55		
TI-RADS	TR 3 ($n = 60$)	5	55	84.8 of TR4 as a cutoff value	83.3 of TR4 as a cutoff value
	TR4 ($n = 37$)	26	11		
	TR5 ($n = 2$)	2	0		
Color Doppler	Avascular (0) ($n = 70$)	15	55	54.5 of intra-nodular vascularity as a cutoff value	100 of intra-nodular vascularity as a cutoff value
	Peri-nodular vascularity (1a) ($n = 11$)	0	11		
	Intra-nodular vascularity (1b) ($n = 15$)	15	0		
	Peri & intra- vascularities (1c) ($n = 3$)	3	0		

[a]*In cases of multiple nodules, the target nodule was considered as the most suspicious one, based on the B-mode and the color Doppler findings in addition to the highest TI-RADS score.*

Table 2 Showing analysis of the elasticity indices of SWE

	Number	Mean	Median	Std deviation	Range	Minimum	Maximum
E_{mean} (kPa)	99	40.1	26.9	29.2	113.9	9.1	123
ER	2.53	3.1	1.9	2.3	8	1.0	9.0

E_{mean}: the mean elasticity index of the stiffest portion of the nodule, *ER* the ratio of mean elasticity index of the lesion and parenchyma or surrounding sternocleidomastoid muscle

- *Inclusion criteria*: Patients with suspicious thyroid nodules (solid or partially solid; based on the clinical and US examinations) who were referred for FNCA
- *Exclusion criteria*: Patients with an abnormal bleeding profile or those who had only diffuse thyroid disease but no existing nodules, also those who had pure cystic nodules

This study was conducted following the ethical guidelines of the Research Ethics Committee of our institute (reference number: Code D-24-2019; date of approval 13-07-2019), and it was approved. All the participants were informed of the details and gave their written informed consent.

All of our patients were subjected to the following:

Conventional ultrasound and shear wave elastography
B-mode and color Doppler examinations were done traditionally for assessing the number, size, composition, echogenicity, shape, margin, and calcification of the nodules (Table 1). Then, the nodules were scored according to ACR TI-RADS criteria [10].

Vascularity-wise, the examined nodules were classified accordingly into avascular nodules (0), nodules with peripheral vascularity (1a), nodules with internal vascularity (1b), and nodules with both peripheral and internal vascularities (1c) (Table 1).

TOSHIBA Aplio 500 machine (equipped with a 7.5-MHz linear probe) was used.

Shear wave examination was subsequently done by the same operator (who is a 3-year experienced subject with the US and elastography techniques) for target nodules using the same US machine and probe. After identification of the lesion, the transducer was kept in a stable perpendicular position without pressure for 3 s to minimize the compression artifact.

Shear wave mode was applied over the B-mode image. A color signal box of appropriate size was displayed as a colored area, where softer areas were blue, and the harder areas were red. Whenever the cine loop was stable by showing parallel lines or parallel circles (free of dot artifacts or zigzag lines), we froze the image and started the interrogation process.

Elastographic quantitative assessment was done using a suitable region of interest (ROI), that was placed in the stiffest region, but avoiding the cystic components, visible calcifications, and the surrounding blood vessels.

The average SWE values in the selected ROI were recorded in kilo Pascal (kPa) for each lesion. A second ROI of the appropriate size was placed in the normal thyroid parenchyma or on the sternocleidomastoid muscle to obtain the elastic ratio (ER), which is the mean stiffness for the lesion-to-normal parenchyma. Repeating the process (at least three successive measurements) was performed for the nodule to choose the best SWE image. If a large nodule was present, multiple measurements for different regions were done.

Ultrasound-guided fine-needle aspiration and cytological examination (FNAC)
The suspicious nodules were localized and aspirated under US image using a 20–22G needle after sterilization without local anesthesia. At least five slides were obtained for the cytological analysis. The samples were immediately smeared and fixed in 95% ethanol. The slides were stained, examined, and analyzed by an expert cytopathologist using the six-tiered diagnostic *Bethesda system* [11].

Thyroid surgery was tailored and performed according to the cytological and clinical diagnoses. It was performed in only 72 cases, who had suspicious nodules (*Bethesd a 4 & 5*), had benign nodules (*Bethesda 2*) but causing compressive or clinical symptoms, or those who had cytological results of undetermined significance (*Bethesda 3*).

Table 3 Showing correlation between SWE and the pathological results of the nodules

Histopathology	E_{mean} (kPa)	Minimum E_{mean} (kPa)	Maximum E_{mean} (kPa)	Number
Benign	24.5 ± 12.1	9.1	58	66
Malignant	69.4 ± 27.02	22	123	33
Total	39.5 ± 28.09	9.1	123	99

Table 4 Showing diagnostic performance of SWE parameters

Elasticity indices (kPa)	AUC% (95% CI)	p value	Cutoff values (kPa)	Sensitivity (%)	Specificity (%)
E_{mean}	93.2 (88.2–98.2)	< 0.0001	34.35	84.8	83.3
ER	96.3 (93.3–99.4)	< 0.0001	2.65	90.9	89.4

AUC area under the curve, *95% CI* 95% confidence interval

Statistical methods and data analysis

Data management and analysis were performed using a statistical package for Social Sciences (SPSS) version 25 for Windows [12].

The numerical data were statistically presented in terms of median, range, or mean, and standard deviation. Categorical data were summarized as numbers and percentages. A comparison between numerical variables was done by Student's unpaired *t* test or Mann–Whitney *U* test for parametric data. Comparing categorical variables was done by Chi-square test or Fisher exact test.

The diagnostic performance of SWE elasticity indices (EIs) and TI-RADS scores was assessed by analyzing receiver operating characteristic (ROC) curves for predicting malignancy, optimal SWE cutoff values, and TI-RADS scores. The *p* value was considered significant when *p* values are less than 0.05.

Results

The obtained results could be binned into six items as follows:

Analysis of conventional ultrasound and color Doppler characteristics of the nodules (Table 1)

We had found no significant correlation between the size, number, or site of the nodules and the possibility of malignancy (*p* value > 0.05).

We found that hypo or marked hypoechogenicity was the most significant single B-mode ultrasound criterion for malignancy; however, TI-RADS had a higher sensitivity in the detection of malignancy than the single US criterion alone.

Table 5 Showing cytological results of the nodules according to Bethesda classification

Bethesda category	Frequency	Valid percent
2	47	47.5
3	4	4.0
4	18	18.2
5	28	28.3
6	2	2.0
Total	99	100

Table 6 Showing the pathological results after FNAC ± surgery

Pathology	Frequency	Valid percent
Benign	66	66.7
Malignant	33	33.3
Total	99	100

Color Doppler had shown an important role in the detection of malignancy, where the presence of intra-nodular vascularity (type 1b) (Table 1) was more specific to malignant nodules but its absence cannot exclude malignancy (Figs. 5 and 6).

Shear wave elastography of the nodules (Tables 2, 3, and 4)

We had detected that E mean and ER of SWE were significantly higher in malignant nodules than in benign nodules (*p* < 0.001). As compared with the other SWE parameters, ER with the optimal cutoff value set at 2.6 had the highest AUC value (96.3%; 95% CI 93.3–99.4%), showing a diagnostic sensitivity and specificity of 90.9 and 89.4%, respectively.

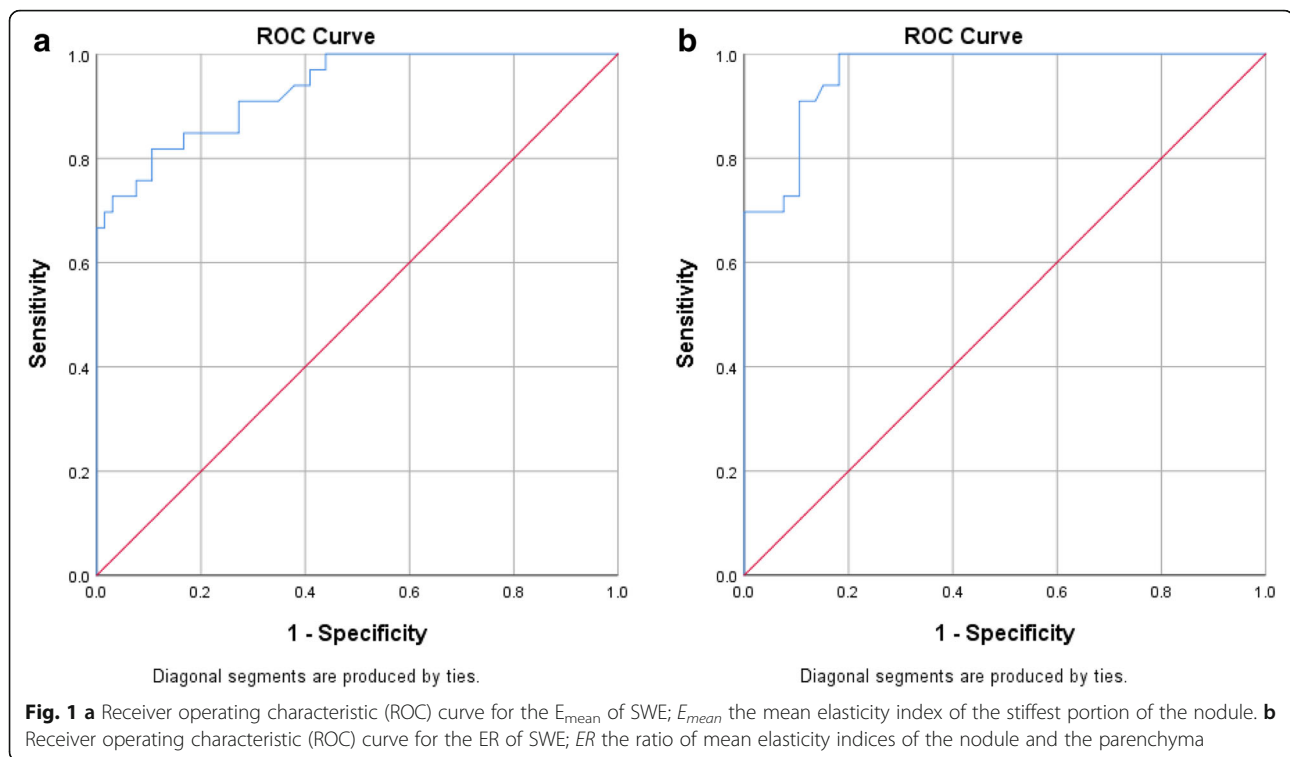### Cytological ± histopathological analysis of the nodules (Table 5, 6, and 7) (Fig. 1 a and b)

From the combined results of FNAC and surgery, we had 66 benign nodules (Figs. 2 and Fig. 3) consisting of 41 nodules of benign nodular goiter, 10 nodules of chronic lymphocytic thyroiditis (Fig. 4), and 15 nodules of follicular adenoma. Alternatively, there were 33 malignant nodules, consisting of 24 nodules of papillary carcinoma (Figs. 5 and 6), five nodules of follicular carcinoma, three nodules of medullary carcinoma (Fig. 7), and only one nodule that was anaplastic undifferentiated carcinoma.

The malignancy rate and TI-RADS scores in the nodules (Table 8)

Based on our statistics, it has been shown that the malignancy rate and the TI-RADS scores are in a positive

Table 7 Showing the histopathological types of the nodules

Surgery	Frequency	Valid percent
Benign nodular goiter	14	14.1
Chronic lymphocytic thyroiditis	10	10.1
Follicular adenoma	15	15.2
Papillary carcinoma	24	24.2
Follicular carcinoma	5	5.1
Medullary carcinoma	3	3.0
Anaplastic carcinoma	1	1.0
No surgery	27	27.3
Total	99	100

Fig. 1 a Receiver operating characteristic (ROC) curve for the E_{mean} of SWE; E_{mean} the mean elasticity index of the stiffest portion of the nodule. **b** Receiver operating characteristic (ROC) curve for the ER of SWE; *ER* the ratio of mean elasticity indices of the nodule and the parenchyma

relationship, as the malignancy rate increases with higher TI-RADS scores.

The diagnostic performance of TI-RADS, color Doppler and SWE separately and in combinations (Table 9)

In the "parallel method", when one or both methods (SWE or TI-RADS) resulted in positivity for malignancy, the results were considered positive, and only when both methods resulted in negativity were the results considered negative.

Combined application of color Doppler and TI-RADS as well as SWE and TI-RADS (Table 9)

Combined color Doppler and TI-RADS score is more significant in terms of sensitivity (87.8%), NLR (0.145), and NPV (93.2%), relative to sensitivity (84.8%), NLR (0.182), and NPV (91.6 %) of the TI-RADS alone. On the whole, the "parallel method" using ER of SWE parameters and TI-RADS was more significant in terms of sensitivity (90.9%), NLR (0.12), and NPV (94.2%), relative to sensitivity (84.8%), NLR (0.182), and NPV (91.6 %) of the TI-RADS alone. Finally, the "parallel" using E_{mean} of SWE and TI-RADS was more significant in terms of sensitivity (90.9%), NLR (0.12), and NPV (94.2%), which were superior to sensitivity (84.8%), NLR (0.182), and NPV (91.6 %) of each TI-RADS or SWE E_{mean} when either used alone.
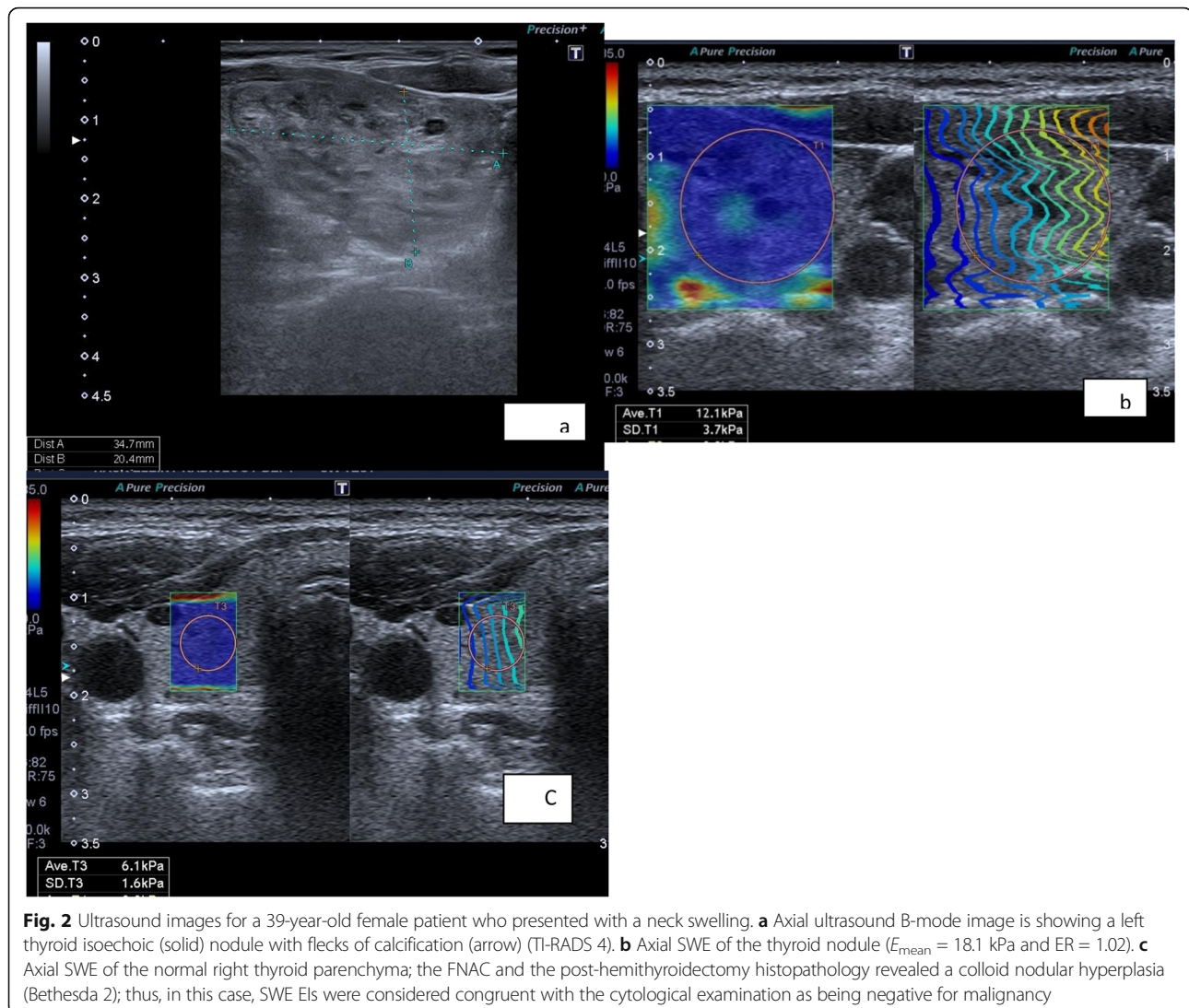
Discussion

The prevalence of thyroid nodules has necessitated the differentiation between benign and malignant ones. As the clinical examination cannot provide a definitive diagnosis, thus, ultrasonography and radioisotope scanning were employed for sorting out the nodules that should be further assessed by histopathology [9].

The sonographic appearance of suspicious nodules can predict the need for histopathological evaluation of them. The US elastography can provide an objective assessment of tissue stiffness [6].

In this context, our results had outlined the most predictive US feature of malignancy by B-mode, as hypo or marked hypo-echogenicity, with the highest sum of the sensitivity and specificity (66.6 and 90.9%, respectively), and this was incongruent with Zhao et al. [13] who had described the micro-calcification as being the most predictive US feature of malignancy (85% sensitivity and 75.6% specificity); this difference is explained by the different sample sizes, where they had a larger sample (313 patients) and a relatively larger number of malignant nodules (194).

From the above and in concordance with Sibos study [14], there is no single US criterion that carries sufficiently high accuracy measures in distinguishing the nodules, but the combination of multiple criteria could increase the sensitivity and specificity.
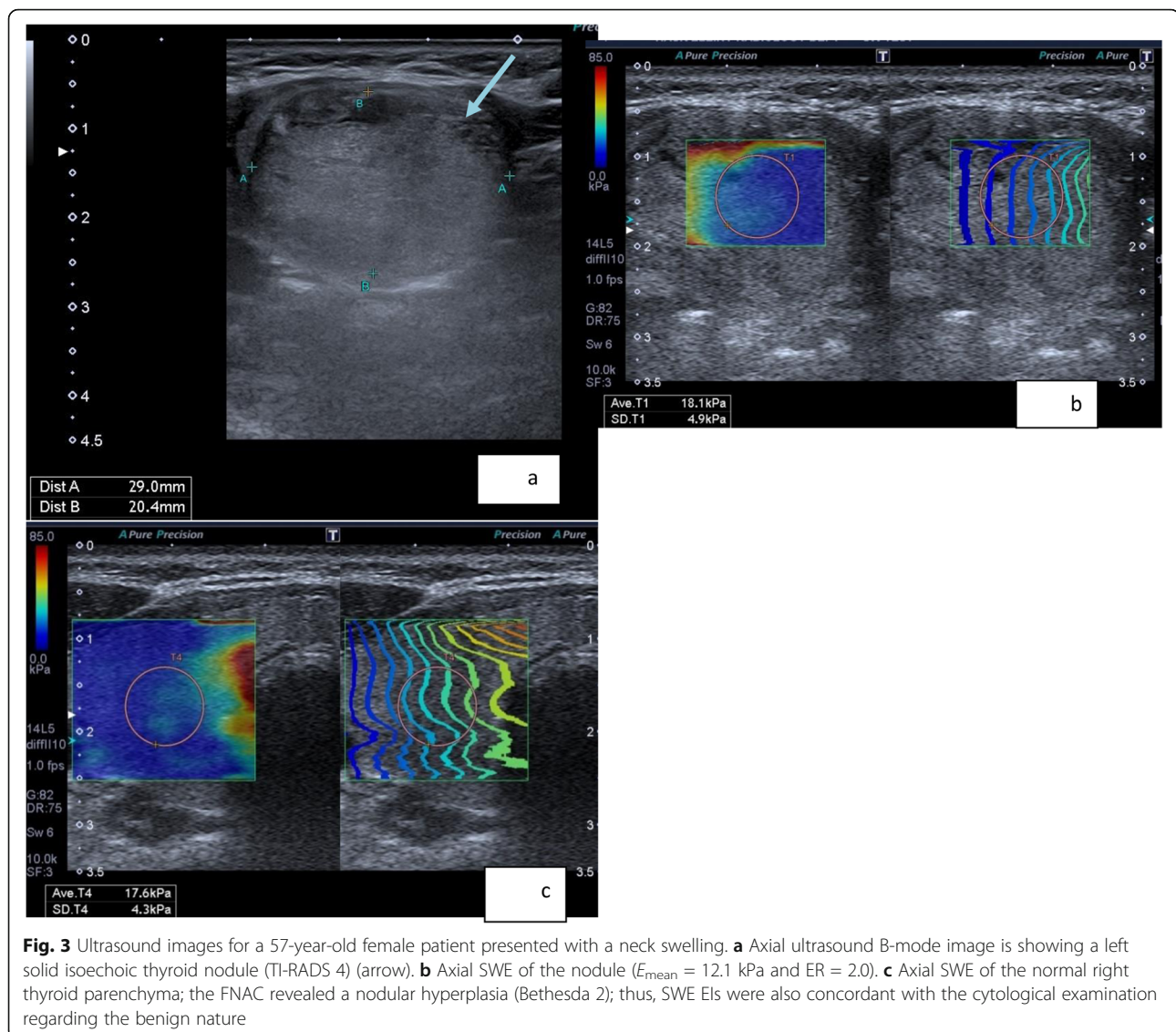
Fig. 2 Ultrasound images for a 39-year-old female patient who presented with a neck swelling. **a** Axial ultrasound B-mode image is showing a left thyroid isoechoic (solid) nodule with flecks of calcification (arrow) (TI-RADS 4). **b** Axial SWE of the thyroid nodule (E_{mean} = 18.1 kPa and ER = 1.02). **c** Axial SWE of the normal right thyroid parenchyma; the FNAC and the post-hemithyroidectomy histopathology revealed a colloid nodular hyperplasia (Bethesda 2); thus, in this case, SWE Els were considered congruent with the cytological examination as being negative for malignancy

Horvath et al. [15] had introduced the TI-RADS for risk stratification of thyroid malignancy. Their tested sensitivity was 88%, and NPV was 88%; Russ et al. [16] had also reported high sensitivity (95.7%) and NPV (99.7%) for diagnosing thyroid malignancy by TI-RADS, then Tessler et al. [10] had updated the TI-RADS scoring; the latter was used in our study with the pooled sensitivity and NPV of TI-RADS (in our study) of 84.8 and 91.6%, respectively.

The ROC curves—in our study—had indicated that the cutoff value of ACR TI-RADS was TR4, and the AUC was 0.84 (95%CI 0.754–0.907) with the diagnostic sensitivity and specificity of ACR TI-RADS of 84.8% and 83.3%, respectively; this was concordant with Zhang et al. [17], where their cutoff value for the ACR TI-RADS was TR5, and AUC was 0.864 (95%CI 0.879–0.934) (81.4% sensitivity and 84.8% specificity); Xu et al.

[18] also had reported an approximate cutoff point for malignancy by ACR TI-RADS, which was more than TR4 (80.6% sensitivity, 78.4% specificity, and 79.6% accuracy of the average value).

By using the color Doppler, we had noticed that the presence of intra-nodular vascularity (Type 1b) was close to the possibility of malignancy, but simultaneously, the presence of the peri-nodular vascularity or avascular nodules cannot exclude it, so the color Doppler solely had a limited role in the differentiation between the thyroid nodules; however, in congruence with Manoj et al. [19], we found that (1b) pattern was the cutoff value for the suggestion of malignancy with 54.5% sensitivity, 100% specificity, and 81.4% NPV.

Shear wave elastography is one of the elastography techniques that had gained a high sensitivity and

Fig. 3 Ultrasound images for a 57-year-old female patient presented with a neck swelling. **a** Axial ultrasound B-mode image is showing a left solid isoechoic thyroid nodule (TI-RADS 4) (arrow). **b** Axial SWE of the nodule (E_{mean} = 12.1 kPa and ER = 2.0). **c** Axial SWE of the normal right thyroid parenchyma; the FNAC revealed a nodular hyperplasia (Bethesda 2); thus, SWE EIs were also concordant with the cytological examination regarding the benign nature

specificity for evaluation of the thyroid nodules and can decrease the unnecessary invasive procedures [9, 20].

We had found that EIs were significantly higher in malignant thyroid nodules than in benign ones (p < 0.0001), this was stated in the meta-analysis study done by Peiliang et al. (84.3% sensitivity and 88.4% specificity) [21].

Hye et al. [22] had reported higher EIs in thyroid carcinoma relative to the benign nodules with E_{mean} with diagnostic specificity of 86.4% and PLR of 4.2; this is nearly compatible to our study, where, the E_{mean} had a diagnostic specificity of 83.3% and PLR of 5.09.

Among the tested SWE EIs, we had selected the elasticity ratio (ER) as the best cutoff value because it has the highest sensitivity and specificity values in the differentiation between the malignant and the benign thyroid nodules. The ER cutoff value of 2.6 had the highest AUC value (96.3%; 95% CI 93.3–99.4%); it had a sensitivity, specificity, PLR, PPV, and NPV of 90.9, 89.4, 8.5, 81, and 85.1%, respectively.

Although matching Veyrieres et al. [23], Bhatia et al. [24], Sebag et al. [25], and Kim et al. [26] studies, up to our knowledge, the most accurate cutoff value of SWE has not yet been unified. This difference between the studies may be attributed to the choice of different standards. We had selected the best cutoff value in ER (which was 2.6), whereas they had used the best parameter that gave a NPV or a PPV of at least 80%.

Consistent with this rule in the selection of the best cut-off value, many published studies over the past years are concordant with us, including Liu et al. [27], Park et al. [28], Zhao et al. [13], and Zhang et al. [17], where

Fig. 4 Ultrasound images for a 55-year-old male patient. **a** Axial ultrasound B-mode image is showing a right solid heterogeneous thyroid nodule (TI-RADS 3). **b** Axial SWE of the thyroid nodule (E_{mean} = 21.2 kPa and ER = 1.6). **c** Axial SWE of the normal right sternocleidomastoid muscle; the FNAC revealed abundant lymphocytic cells with scanty follicular cells (Bethesda 2), and the post total thyroidectomy histopathological results had confirmed the diagnosis of chronic lymphocytic thyroiditis; thus, SWE EIs were matching the cytological examination

they had also considered that the EIs are significantly higher in malignant nodules with high accuracy measures.

Adding to our knowledge, two important salient findings—in our study—were demonstrated where the combination of SWE and TI-RADS as well as color Doppler and TI-RADS to a certain extent had increased the diagnostic performance in differentiating thyroid nodules. Moreover, when we used the SWE (ER) and TI-RADS, we had obtained higher accuracy measures compared with the TI-RADS alone; therefore, such a combination of TI-RADS and EIs can minimize the need for unnecessary surgery or biopsy in suspicious thyroid nodules; this was concordant with Park et al. [28], Zhao et al. [13], and Xu et al.'s [18] studies, where the combined use of the TI-RADS findings and the EIs had increased the accuracy measures.

However, it had been shown that the rise in the sensitivity was from 84.8% of TI-RADS alone to 90.9% with the combination of TI-RADS and SWE in "parallel" but the specificity was lower (74.2%) as compared with TI-RADS alone (83.3%); this was explained by the statistical way in which we chose the positive cases of possible malignancy as we use the parallel method when one or both methods had resulted in positivity, and the results were considered negative when only both methods had resulted in negativity; this relationship between both methods is termed "parallel"; and it can explain why the sensitivity is higher while the specificity is lower in the combined method than in TI-RADS alone.

Finally, from our results, we had found that the SWE and TI-RADS can form a complementary relationship in terms of the advantages. Where the TI-RADS can compensate for the limitations of SWE (that may be disturbed by macro-calcifications and the carotid artery
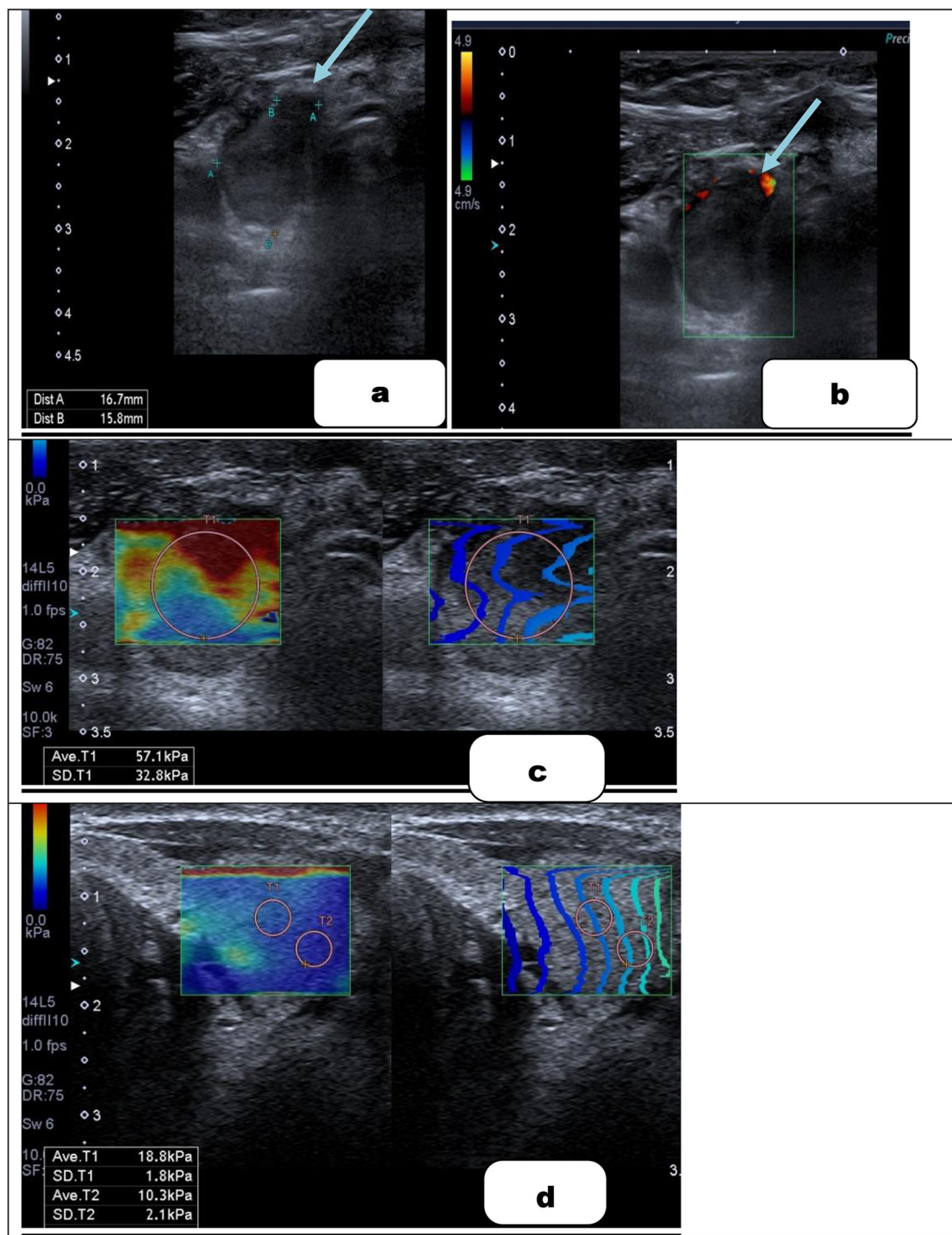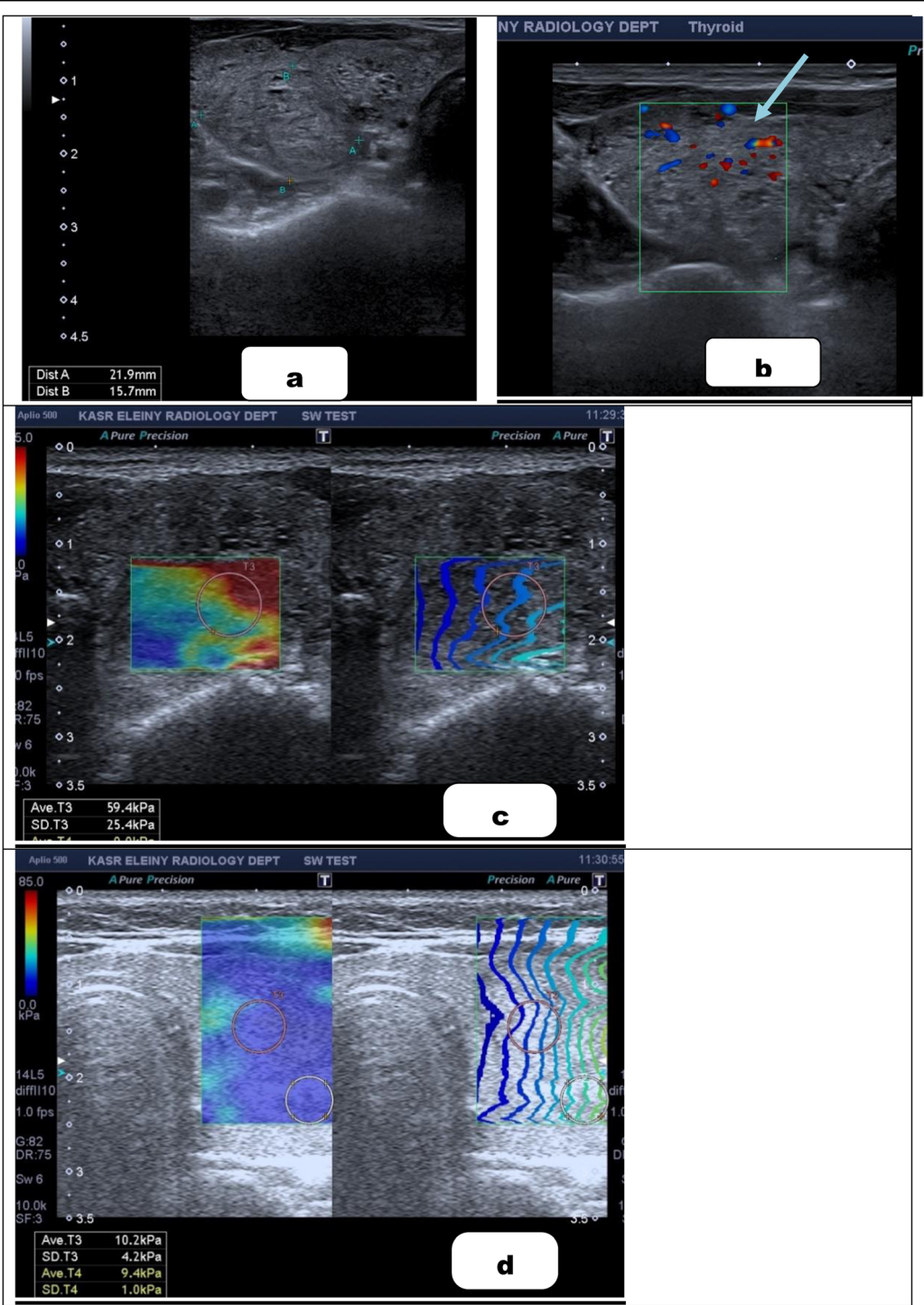
Fig. 5 Ultrasound images for a 60-year-old female patient. **a** Axial ultrasound B-mode image is showing a right solid hypoechoic thyroid nodule with an irregular margin and peripheral calcification (TI-RADS 5) (arrow). **b** Axial color image is showing peripheral vascularity (1a) (arrow). **c** Axial SWE of the thyroid nodule (E_{mean} = 57.0 kPa and ER = 3). **d** Axial SWE of normal left thyroid parenchyma; the FNAC revealed malignant cells with psammoma bodies (Bethesda 5), and the post right hemithyroidectomy histopathology had confirmed the diagnosis of papillary thyroid carcinoma

pulsations) and vice versa, the SWE can compensate for TI-RADS, which can be influenced by the operator dependence and the interobserver variability. Thus, we suggest using SWE for the thyroid nodules with TI-RADS score greater than or equal to 4 as a complementary tool, other than doing the diagnosis separately to

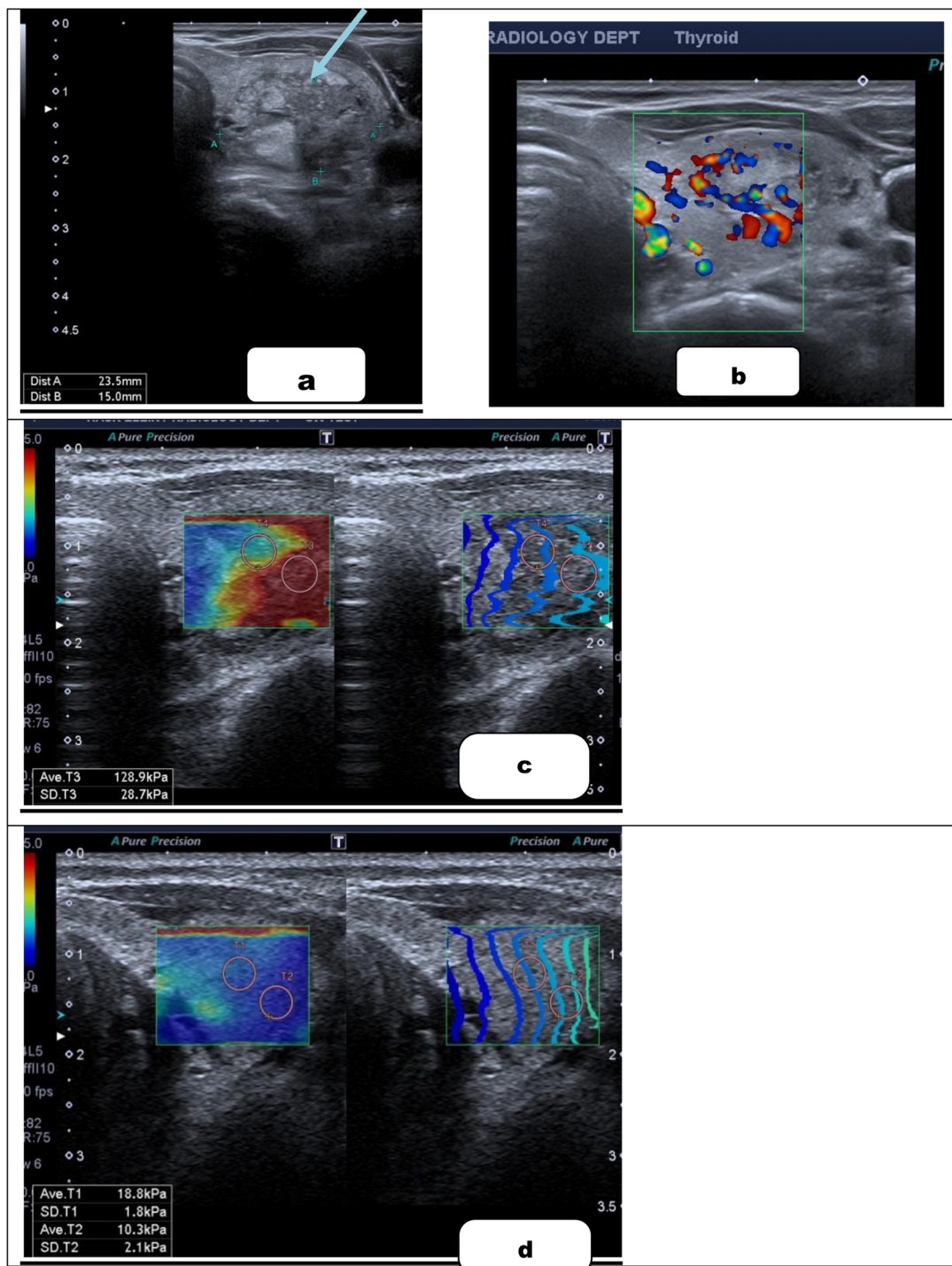**Fig. 6** Ultrasound images for a 58-year-old female patient. **a** Axial ultrasound B-mode image is showing two solid thyroid nodules that are isoechoic with calcification (TI-RADS 5). **b** Axial color image is showing internal vascularity (1b) (arrow). **c** Axial SWE of the thyroid nodule (E_{mean} = 59.4 kPa and ER = 5.8). **d** Axial SWE of the normal left thyroid parenchyma; the FNAC revealed malignant cells with psammomatous calcification (Bethesda 5), and the post right hemithyroidectomy histopathological examination had confirmed the presence of papillary thyroid carcinoma

Fig. 7 Ultrasound images for a 53-year-old male patient. **a** Axial ultrasound B-mode image is showing heterogeneous left solid thyroid nodules that are hypo to isoechoic with punctuate and macro calcification (TI-RADS 4) (arrow). **b** Axial color image is showing both peripheral and internal vascularity (1c). **c** Axial shear wave elastography of the thyroid nodule (E_{mean} = 128.9 kPa and ER = 6.8). **d** Axial SWE of the normal right thyroid parenchyma; the FNAC revealed malignant cells with psammomatous calcification (Bethesda 5), and the post total thyroidectomy histopathological examination had confirmed the presence of medullary thyroid carcinoma

Table 8 Showing the malignancy rate according to the TI-RADS score of the 99 nodules after FNAC ± thyroid surgery

TI-RADS score	No. of cases	Benign	Malignant	Malignancy rate (%)
3	60	55	5	8.3
4	37	11	26	70.3
5	2	0	2	100
Total	99	66	33	

avoid unnecessary invasive diagnostic procedures in suspicious nodules.

Some limitations had been met in this work including the following:

First, all malignant nodules (24/33) were papillary carcinomas, while only three nodules were medullary carcinomas, and most of the benign nodules were nodular goiters; thus, other pathological types were not included, such as Hurthle cell thyroid carcinoma and primary thyroid lymphoma; thus, their tested parameters were not examined in this study.

Second, it is a one-center experience, so the data need to be tested by prospective multicenter and nonspecialized members to eliminate this selection bias.

Third is the isthmic lesions, where the relatively small size of the isthmus compared with the thyroid lobes and the ROI should cover the whole nodule with sufficient surrounding parenchyma are needed; however, isthmic lesions were seen in 10 of our cases, most of them were "isthmi-lobar" in location, thus surrounding thyroid parenchyma served to avoid this limitation; however, in pure isthmic lesions, breath-holding and cessation of

swallowing as well as the application of a copious amount of gel is considered of paramount importance, moreover, repeating the process, where at least 3 successive measurements were taken for each nodule to choose the best SWE image.

Forth, is the inter\intra-observer variability and the operator dependency, this was much lessened by conducting the examinations using the same US machine at the same setting of the conventional US examination, and by the same operator under the direct supervision of an experienced senior.

Last, selection bias may exist because patients included in our study were scheduled for US-guided FNAC for suspicious thyroid nodules with US features (TR ≥ 3), this may decrease the diagnostic performance on TI-RADS, causing false-negative cytologic results.

Finally, it would be interesting to see any solid and conclusive results that can lead to a change in practice as the researches about the SWE are there and giving promising results for a long time, but it is not included in any known thyroid scoring systems so far.

Table 9 Showing a comparison of diagnostic performance of TI-RADS alone, SWE alone, color Doppler alone, and the combined parallel method

Imaging method		Malignant	Benign	AUC%	Sensitivity	Specificity	PLR	NLR	PPV	NPV
TI-RADS alone (4 as a cutoff value)	+	28	11	84 (75.4–90.7)	84.8	83.3	5.09	0.182	71.7	91.6
	−	5	55							
Color Doppler alone (1b as a cutoff value)	+	18	0	77 (67.8–85.1)	54.5	100		0.45	100	81.4
	−	15	66							
SWE alone (ER 2.6 as a cutoff value)	+	30	7	96 (93.3–99.4)	90.9	89.3	8.5	0.10	81.08	95.1
	−	3	59							
SWE alone (E_{mean} 34.3 as cutoff value)	+	28	11	84 (75.4–90.7)	84.8	83.3	5.09	0.182	71.7	91.6
	−	5	55							
Combined TIRADS & color Doppler		29	11	85 (77.1–91.9)	87.8	83.3	5.2	0.145	72.5	93.2
		4	55							
Combined TIRADS + SWE (ER)	+	30	17	#	90.9	74.2	3.5	0.12	63.8	94.2
	−	3	49							
Combined TIRADS + SWE (E_{mean})	+	30	21	#	90.9	68.1	2.8	0.133	58.8	93.7
	−	3	45							

AUC, areas under the ROC curve; *PLR*, positive likelihood ratio; *NLR*, negative likelihood ratio; *PPV*, positive predictive value; *NPV*, negative predictive value; *95% CI*, 95% confidence interval
+ stands for positivity for malignancy, − stands for negativity for malignancy, # stands for not applicable

Conclusion

Elasticity indices had shown a significantly high diagnostic value that is comparable to the histopathological results. Combined SWE, color Doppler, and TI-RADS could effectively complement each other in the differentiation between the thyroid nodules as a sum of findings. Furthermore, the combined method could be used as a simple and non-invasive tool that accurately stratifies the risk of malignancy and surrogates the invasive diagnostic procedures.

Abbreviations

EIs: Elasticity indices; E_{mean}: The mean elasticity index of the stiffest portion of the nodule; ER: The ratio of mean elasticity index of the lesion and the normal parenchyma or subjacent sternocleidomastoid muscle; FNAC: Fine-needle aspiration cytology; SWE: Shear wave elastography; TI-RADS: Thyroid imaging reporting and data system

Authors' contributions

AAB, the corresponding author, had contributed by supervising the ultrasound examinations and in the final editing and submission of the manuscript. AHMA had done the ultrasound examinations for the patients and shared in the manuscript editing and reference collection. YFG had reported the histopathology findings for the sampled cases. KHE had introduced the idea of the current study and helped in the image selection and revised the final version of the submitted manuscript. The authors have read and approved the manuscript.

Availability of data and materials

All data are available on a software system owned by each of the authors, and the corresponding author has the authority to respond if there is any query.

Declarations

Ethics approval and consent to participate

The protocol was reviewed and approved by the local ethics committee of the radiology department, Kasr Alainy Hospital, Cairo University (reference number: Code D-24-2019, Date of approval 13-07-2019). All patients had given their written consents to participate in this work.

Consent for publication

All patients had given their written consents for publication of this work.

Competing interests

All authors have no competing interests.

Author details

[1]Radiology Department, Faculty of Medicine, Cairo University, Cairo, Egypt. [2]Radiology Departement , Faculty of Medicine, Cairo University, Cairo, Egypt.

References

1. Mcnicol A (2007) Pathology of thyroid tumors. Surg Oxford 25(11):458–462
2. Hegedüs L, Steen JB et al (2003) Management of simple nodular goiter: current status and future perspectives. Endocrine Rev 24(1):102–132. https://doi.org/10.1210/er.2002-0016
3. Frates MC, Benson CB, Charboneau JW, Cibas ES, Clark OH, Coleman BG, Cronan JJ, Doubilet PM, Evans DB, Goellner JR, Hay ID, Hertzberg BS, Intenzo CM, Jeffrey RB, Langer JE, Larsen PR, Mandel SJ, Middleton WD, Reading CC, Sherman SI, Tessler FN, Society of Radiologists in Ultrasound (2005) Management of thyroid nodules detected at US: Society of Radiologists in Ultrasound consensus conference statement. Radiology 237(3):794–800. https://doi.org/10.1148/radiol.2373050220
4. Wynford-Thomas D (1993) Molecular genetics of thyroid cancer. Trends Endocrinol Metab 4(7):224–232. https://doi.org/10.1016/1043-2760(93)90126-Y
5. Kwak JY, Kim EK (2014) Ultrasound elastography for thyroid nodules: recent advances. Ultrasonography 33(2):75–82. https://doi.org/10.14366/usg.13025
6. Cantisani V, Lodise P, Grazhdani H, Mancuso E, Maggini E, di Rocco G, D'Ambrosio F, Calliada F, Redler A, Ricci P, Catalano C (2014) Ultrasound elastography in the evaluation of thyroid pathology. Current status. Eur J Radiol 83(3):420–428. https://doi.org/10.1016/j.ejrad.2013.05.008
7. Abdel Razek AA (2010) Diffusion-weighted magnetic resonance imaging of head and neck. J Comput Assist Tomogr 34(6):808–815
8. Shokry A, Hassan T, Baz A et al (2018) Role of diffusion-weighted magnetic resonance imaging in the differentiation of benign and malignant thyroid nodules. Egypt J Radiol Nuclear Med 49(4):1014–1021. https://doi.org/10.1016/j.ejrnm.2018.06.013
9. Nell S, Kist JW, Debray TP et al (2015) Qualitative elastography can replace thyroid nodule fine-needle aspiration in patients with soft thyroid nodules. A systematic review and meta-analysis. Eur J Radiol. 84(4):652–661. https://doi.org/10.1016/j.ejrad.2015.01.003
10. Tessler F, Middleton W, Grant E et al (2017) ACR Thyroid Imaging, Reporting and Data System (TI-RADS): white paper of the ACR TI-RADS committee. J Am Coll Radiol 14(5):587–595. https://doi.org/10.1016/j.jacr.2017.01.046
11. Cibas ES, Ali SZ (2007) The Bethesda system for reporting cytopathology. Thyroid. 19(11):1159–1165
12. Galen RS (1980) Predictive values and efficiency of laboratory testing. Pediat J Clin North Am 27(4):861–869. https://doi.org/10.1016/S0031-3955(16)33930-X
13. Zhao L, Hui J, Xue H et al (2017) Shear wave elastography combined with the thyroid imaging reporting and data system for malignancy risk stratification in thyroid nodules. Oncotarget journal. January. 8(26): 43406–43416
14. Sipos JA (2009) Advances in ultrasound for the diagnosis and management of thyroid cancer. Thyroid (19):1363–1372
15. Horvath E, Majlis S, Rossi R et al (2009) An ultrasonogram reporting system for thyroid nodules stratifying cancer risk for clinical management. J Clin Endocrinol Metab (94):1748–1751
16. Russ G, Royer B, Bigorgne C, Rouxel A, Bienvenu-Perrard M, Leenhardt L (2013) Prospective evaluation of thyroid imaging reporting and data system on 4550 nodules with and without elastography. Eur J Endocrinol 168(5): 649–655. https://doi.org/10.1530/EJE-12-0936
17. Zhang W-B, Li JJ et al (2020) SWE combined with ACR TI-RADS categories for malignancy risk stratification of thyroid nodules with indeterminate FNA cytology, pp 1–10
18. Xu X, He X, Guo L et al (2019) The diagnostic value of the maximum value of Young's modulus of shear-wave elastography and ACR TI-RADS for thyroid nodules. J Clin Otorhinolaryngol. 33(8):764–767
19. Manoj KP, Senthil KA, Upasana R et al (2016) Role of gray scale, color Doppler, and spectral Doppler in differentiation between malignant and benign thyroid nodules. J Clin Diagnosis Res 10(8):01–06
20. Binglan Z, Xuelei M, Nana W et al (2013) Shear wave elastography for differentiation of benign and malignant thyroid nodules: a meta-analysis. J Ultrasound Med (32):2163–2169
21. Peiliang L, Chen M, Liu B et al (2014) Diagnostic performance of shear wave elastography in the identification of malignant thyroid nodules: a meta-analysis. EurRadiol 24:2729–2738
22. Hye JK, Mi KK, In HC et al (2019) Utility of shear wave elastography to detect papillary thyroid carcinoma in thyroid nodules: efficacy of the standard deviation elasticity. Korean J Intern Med. 34(4):850–857
23. Veyrieres JB, Albarel F, Lombard JV et al (2012) A threshold value in shear wave elastography to rule out malignant thyroid nodules: A reality? Eur J Radiol (81):3965–3972
24. Bhatia K, Tong CS, Cho CC, Yuen EH, Lee J, Ahuja AT (2012) Reliability of shear wave ultrasound elastography for neck lesions identified in routine clinical practice. Ultraschall Med 33(5):463–468. https://doi.org/10.1055/s-0032-1325330
25. Sebag J, Vaillant-Lombard BJ et al (2010) Shear wave elastography: a new ultrasound imaging mode for the differential diagnosis of benign and

malignant thyroid nodules. J Clin Endocrinol Metab 95(12):5281–5288. https://doi.org/10.1210/jc.2010-0766

26. Kim H, Kim JA, Son EJ et al (2013) Quantitative assessment of shear-wave ultrasound elastography in thyroid nodules: diagnostic performance for predicting malignancy. EurRadiol (23):2532–2537

27. Liu BX, Xie XY, Liang JY, Zheng YL, Huang GL, Zhou LY, Wang Z, Xu M, Lu MD (2014) Shear wave elastography versus real-time elastography on evaluation thyroid nodules: a preliminary study. Eur J Radiol 83(7):1135–1143. https://doi.org/10.1016/j.ejrad.2014.02.024

28. Park AY, Son EJ, Han K, Youk JH, Kim JA, Park CS (2015) Shear wave elastography of thyroid nodules for the prediction of malignancy in a large scale study. Eur J Radiol. Mar 84(3):407–412. https://doi.org/10.1016/j.ejrad.2014.11.019

Publisher's Note